Molecular Therapy
Original Article

# Inducible Caspase-9 Selectively Modulates the Toxicities of CD19-Specific Chimeric Antigen Receptor-Modified T Cells

Iulia Diaconu,[1] Brandon Ballard,[1] Ming Zhang,[1] Yuhui Chen,[6] John West,[5] Gianpietro Dotti,[1,2,3,5] and Barbara Savoldo[1,4,6]

[1]Center for Cell and Gene Therapy, Baylor College of Medicine, The Methodist Hospital and Texas Children's Hospital, Houston, TX 77030, USA; [2]Department of Medicine, Baylor College of Medicine, The Methodist Hospital and Texas Children's Hospital, Houston, TX 77030, USA; [3]Department of Immunology, Baylor College of Medicine, The Methodist Hospital and Texas Children's Hospital, Houston, TX 77030, USA; [4]Department of Pediatric, Baylor College of Medicine, The Methodist Hospital and Texas Children's Hospital, Houston, TX 77030, USA; [5]Department of Microbiology and Immunology, Lineberger Comprehensive Cancer Center, University of North Carolina, Chapel Hill, NC 27599, USA; [6]Department of Pediatrics, Lineberger Comprehensive Cancer Center, University of North Carolina, Chapel Hill, NC 27599, USA

**Immunotherapy with T cells expressing the chimeric antigen receptor (CAR) specific for the CD19 antigen (CD19.CAR-Ts) is a very effective treatment in B cell lymphoid malignancies. However, B cell aplasia and cytokine release syndrome (CRS) secondary to the infusion of CD19.CAR-Ts remain significant drawbacks. The inclusion of safety switches into the vector encoding the CAR is seen as the safest method to terminate the effects of CD19.CAR-Ts in case of severe toxicities or after achieving long-term sustained remissions. By contrast, the complete elimination of CD19.CAR-Ts when CRS occurs may jeopardize clinical responses as CRS and antitumor activity seem to concur. We have demonstrated, in a humanized mouse model, that the inducible caspase-9 (*iC9*) safety switch can eliminate CD19.CAR-Ts in a dose-dependent manner, allowing either a selective containment of CD19.CAR-T expansion in case of CRS or complete deletion on demand granting normal B cell reconstitution.**

## INTRODUCTION

The adoptive transfer of T cells expressing a chimeric antigen receptor (CAR) specific for the CD19 antigen (CD19.CAR-Ts) promotes potent clinical responses in patients affected by acute lymphoblastic leukemia (ALL)[1–3] and lymphomas.[4] Effective antitumor activity is achieved regardless of the co-stimulation (CD28 versus 4-1BB) provided to the CAR.[2,3] Similarly, side effects of CD19.CAR-Ts encoding either CD28 or 4-1BB, like cytokine release syndrome (CRS) and neurological toxicities, are superimposable.[2–4] Long-term B cell aplasia, the limiting "on target-off tumor" toxicity of CD19.CAR-Ts, strongly correlates with their long-term survival.[2]

Controlling effectively CRS and long-term B cell aplasia, while maintaining potent antitumor activity, are relevant aspects to address prior to introducing CD19.CAR-Ts to the standard practice. The inclusion of safety switches or suicide genes into the vector encoding the CAR is largely seen as the most effective and precise approach to rapidly eliminate CAR-Ts in case of toxicities without causing additional side effects.[5–9] The activation of currently available safety switches produces significant or complete elimination of CAR-Ts and, if included in CD19.CAR-Ts, would assist in terminating their effects to allow the reconstitution of normal B lymphocytes in patients who achieved sustained remission. By contrast, the control of CRS adds complexity to most of the available suicide approaches, as they function as "on-or-off" switches and do not allow any modulation. Being CRS likely interconnected with antitumor effects, the ability to control the symptoms associated with the life-threatening CRS without extinguishing CD19.CAR-T function is required for sustaining the ongoing antitumor activity.[1,2]

The inducible safety switch caspase-9 (*iC9*) is based on a modified human caspase-9 fused to the human FK506 binding protein (FKBP) to grant conditional dimerization using a chemical inducer of dimerization (CID) (AP1903/Rimiducid, Bellicum Pharmaceutical) with consequent apoptosis of cells expressing the fusion protein.[10,11] This safety switch is extremely potent and specific in rapidly eliminating >85%–90% of iC9-tranduced T cells after the administration of one single dose of AP1903.[12–14] While so far clinically used as all classic safety switches to terminate transduced T cells, iC9 is, however, capable of activating ex vivo apoptosis of targeted cells in a dose-dependent fashion upon binding to the CID.[11,15,16] Taking advantage of this unique pharmacological modulation of the iC9-induced apoptosis, we have constructed and validated in vivo in a humanized mouse model a novel CD19.CAR incorporating the *iC9* safety switch (iC9.CD19.CAR-Ts) and showed that iC9 can not only aid in the

Received 2 August 2016; accepted 18 January 2017;
http://dx.doi.org/10.1016/j.ymthe.2017.01.011.

**Correspondence:** Barbara Savoldo, Department of Pediatrics, Lineberger Comprehensive Cancer Center, University of North Carolina, Chapel Hill, NC 27599, USA.
**E-mail:** bsavoldo@med.unc.edu

 

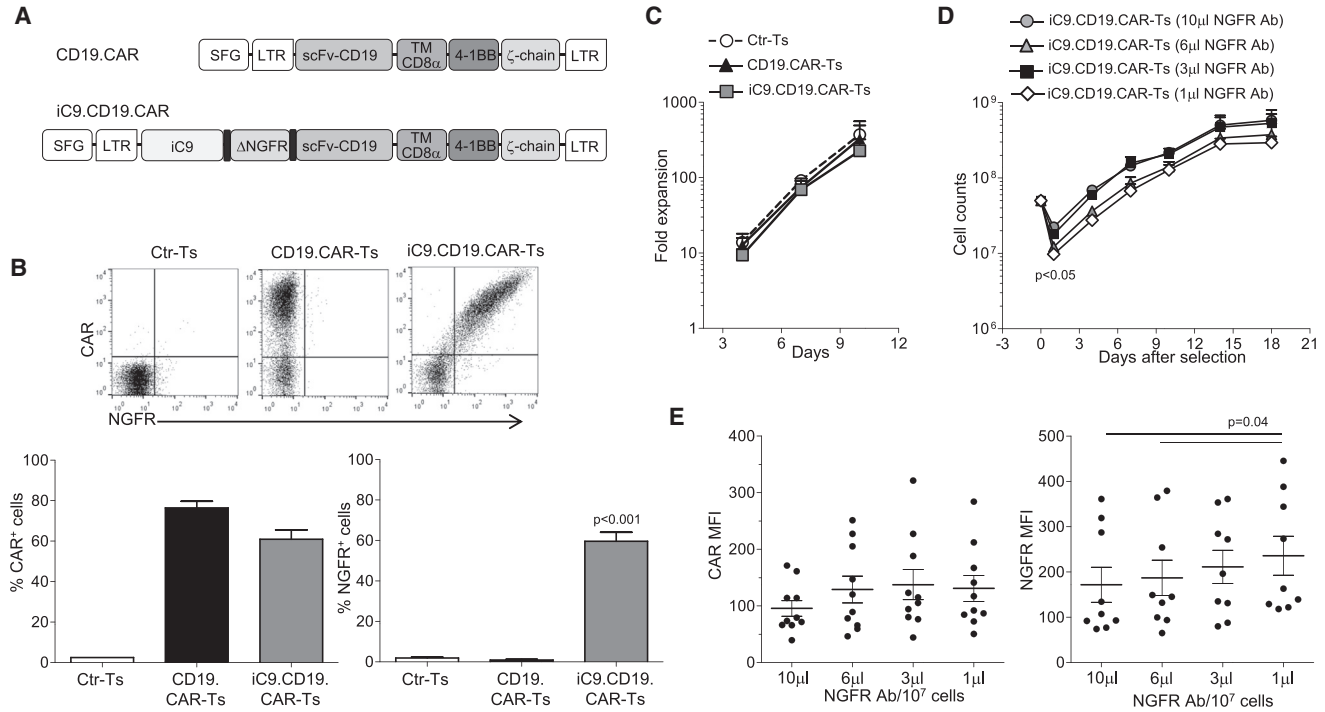


**Figure 1. Generation of Activated T Lymphocytes that Co-express an Inducible Caspase-9, a CD19-Specific CAR, and a Truncated NGFR**

(A) Retroviral constructs used to transduce activated T cells. (B) Flow cytometry plots for CAR and NGFR expression in control T cells (Ctr-Ts), CD19.CAR-Ts, and iC9.CD19.CAR-Ts in a representative experiment (upper panels) and summary of T cell lines generated from six healthy individuals (lower panels). (C) Fold expansion of Ctr-Ts, CD19.CAR-Ts, and iC9.CD19.CAR-Ts. Data are means ± SEM of T cell lines generated from six healthy individuals. (D) T cell counts of iC9.CD19.CAR-Ts selected using the indicated different concentration of NGFR Ab/$10^7$ cells and expanded ex vivo. Data are means ± SEM of T cell lines generated from six healthy individuals. (E) Mean fluorescence intensity (MFI) of CAR and NGFR of T cells selected with the indicated amount of NGFR-PE Ab/$10^7$ cells. Data shown are means ± SEM of T cell lines generated from nine healthy individuals.

on-demand ablation of iC9.CD19.CAR-Ts to allow B cell reconstitution, but also contains the expansion of iC9.CD19.CAR-Ts in case of CRS, without complete elimination of these cells for sustained antitumor activity.

## RESULTS

### Incorporation of a Truncated Form of the Low-Affinity Nerve Growth Factor Receptor Allows Reproducible Selection of iC9.CD19.CAR-Ts

We have previously validated the use of a truncated CD19 molecule in combination with the caspase-9 safety switch as a marker/selection gene both in vitro and in vivo in patients.[12,17] We chose to incorporate in the CAR a truncated *NGFR* as a marker/selection gene, based on its previous clinical validation in combination with the *HSVTK* suicide system and thus availability of clinical grade selection reagents.[18,19] Activated T cells from six healthy donors were transduced with either Ctr or CD19.CAR or iC9.CD19.CAR vectors (Figure 1A) and CAR expression, assessed 3–4 days after viral transduction, was 77% ± 4% and 61% ± 5%, respectively (Figure 1B). Nerve growth factor receptor (NGFR) expression by iC9.CD19.CAR-Ts was similar to CAR expression (60% ± 4%, $p = 0.6$). The expansion rate of both CD19.CAR-Ts and iC9.CD19.CAR-Ts was comparable (Figure 1C). To select iC9.CD19.CAR-Ts, we performed a titration of the primary NGFR-PE antibody (Ab). Specifically, 5 days after transduction, iC9.CD19.CAR-Ts were incubated with increasing concentration of the primary NGFR-PE Ab, ranging from 1 to 10 μL/$10^7$ cells. After immunomagnetic selection, iC9.CD19.CAR-Ts were expanded ex vivo in interleukin-7 (IL-7) and IL-15 cytokines for a total of 18 days. We found that T cell recovery was significantly reduced when lower doses (1 and 3 μL/$10^7$ cells) of NGFR-PE Ab were used, as compared to higher doses (6 and 10 μL/$10^7$ cells; $p < 0.05$). However, after selection, iC9.CD19.CAR-Ts expanded equally well, regardless of the amount of NGFR-PE Ab used (Figure 1D). More than 90% of selected iC9.CD19.CAR-Ts expressed both NGFR and CAR, irrespective of the dose of NGFR-PE Ab used, but, as expected, the MFI of the NGFR was higher in iC9.CD19.CAR-Ts selected with lowest dose of the antibody ($p = 0.04$) (Figure 1E).

### iC9.CD19.CAR-Ts Are Functional In Vitro

We characterized CD19.CAR-Ts and selected iC9.CD19.CAR-Ts to ensure their comparable functions. We found no significant differences in cell memory composition (Figure 2A) or CD4 versus CD8 ratio (data not shown). Similarly, their cytotoxic activity against the

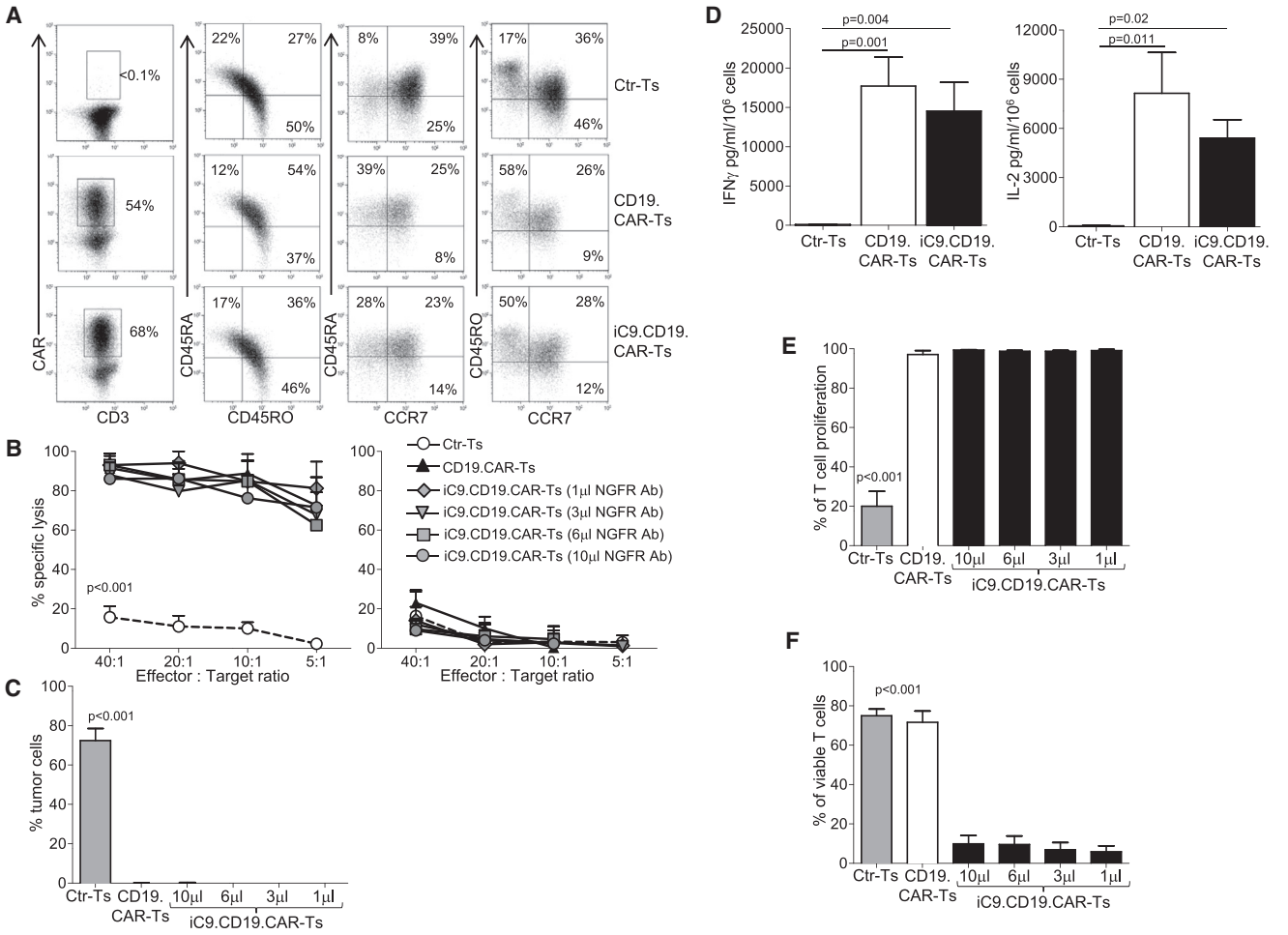


**Figure 2. Functionality In Vitro of iC9.CD19.CAR-Ts**

(A) Immunophenotypic analyses of Ctr-Ts, CD19.CAR-Ts, and iC9.CD19.CAR-Ts for one representative donor. The analysis was performed gating on CAR-expressing cells, except for Ctr-Ts. (B) Cytotoxic activity of Ctr-Ts, CD19.CAR-Ts, and iC9.CD19.CAR-Ts selected using the indicated concentration of the NGFR-PE Ab/$10^7$ cells. Left and right graphs show the percentage of lysis of the $CD19^+$ Raji and the $CD19^-$ K562 cell lines, respectively, in a $^{51}Cr$-based release assay. (C) Percentage of tumor cells in experiments in which $CD19^+$ Raji cells were co-cultured at 1:1 ratio with Ctr-Ts, CD19.CAR-Ts, or iC9.CD19.CAR-Ts selected using the indicated concentration of NGFR-PE Ab/$10^7$ cells. T cells and tumor cells were quantified by flow cytometry. (D) Quantification of IFN-γ and IL-2 released in the supernatant by Ctr-Ts, CD19.CAR-Ts, or iC9.CD19.CAR-Ts co-cultured for 24 hr with $CD19^+$ Raji cells at 1:1 ratio and quantified by Milliplex assay. (E) Percentage of proliferation by Ctr-Ts, CD19.CAR-Ts, and iC9.CD19.CAR-Ts in response to $CD19^+$ Raji cells (ratio 1:1). iC9.CD19.CAR-Ts were selected using the indicated concentration of the NGFR-PE Ab/$10^7$ cells, and T cell proliferation was measured using the CFSE staining. (F) Percentage of viable Ctr-Ts, CD19.CAR-Ts, and iC9.CD19.CAR-Ts after incubation with 10 nM of CID. iC9.CD19.CAR-Ts were selected using the indicated concentration of NGFR-PE Ab/$10^7$ cells and alive cells quantified using the Annexin-V/7-AAD staining. Shown data are means ± SEM of T cell lines generated from six healthy individuals.

$CD19^+$ Raji tumor cells was comparable irrespective of the amount of NGFR-PE Ab used for the selection (Figure 2B), with minimal activity against the $CD19^-$ K562 cells (Figure 2B). Long-term co-culture assays of CD19.CAR-Ts and iC9.CD19.CAR-Ts confirmed comparable antitumor activity, with complete elimination of $CD19^+$ Raji tumor cells by day 5 of co-culture (Figures 2C and S1A). From the same co-cultures, cytokines were measured in supernatant collected after 24 hr incubation, and no differences in IL-2 or interferon (IFN)-γ release were observed (Figures 2D and S1B). Of note, no specific release of IL-6 was found by CAR-Ts in response to the specific antigen (Figure S1B), suggesting, as previously described,[20] that, in patients experiencing CRS, IL-6 is unlikely produced by CAR-Ts. Similarly, CD19.CAR-Ts and iC9.CD19.CAR-Ts showed comparable proliferative capacity in response to $CD19^+$ Raji cells (Figures 2E and S1C), confirming that the inclusion of the iC9 does not adversely affect CAR-T characteristics. Finally, we tested the function of the iC9 component by incubating iC9.CD19.CAR-Ts with 10 nM of CID. Less than 10% viable cells were detected after 24 hr incubation, irrespective of the dose of NGFR-PE Ab used (Figures 2F and S1D).

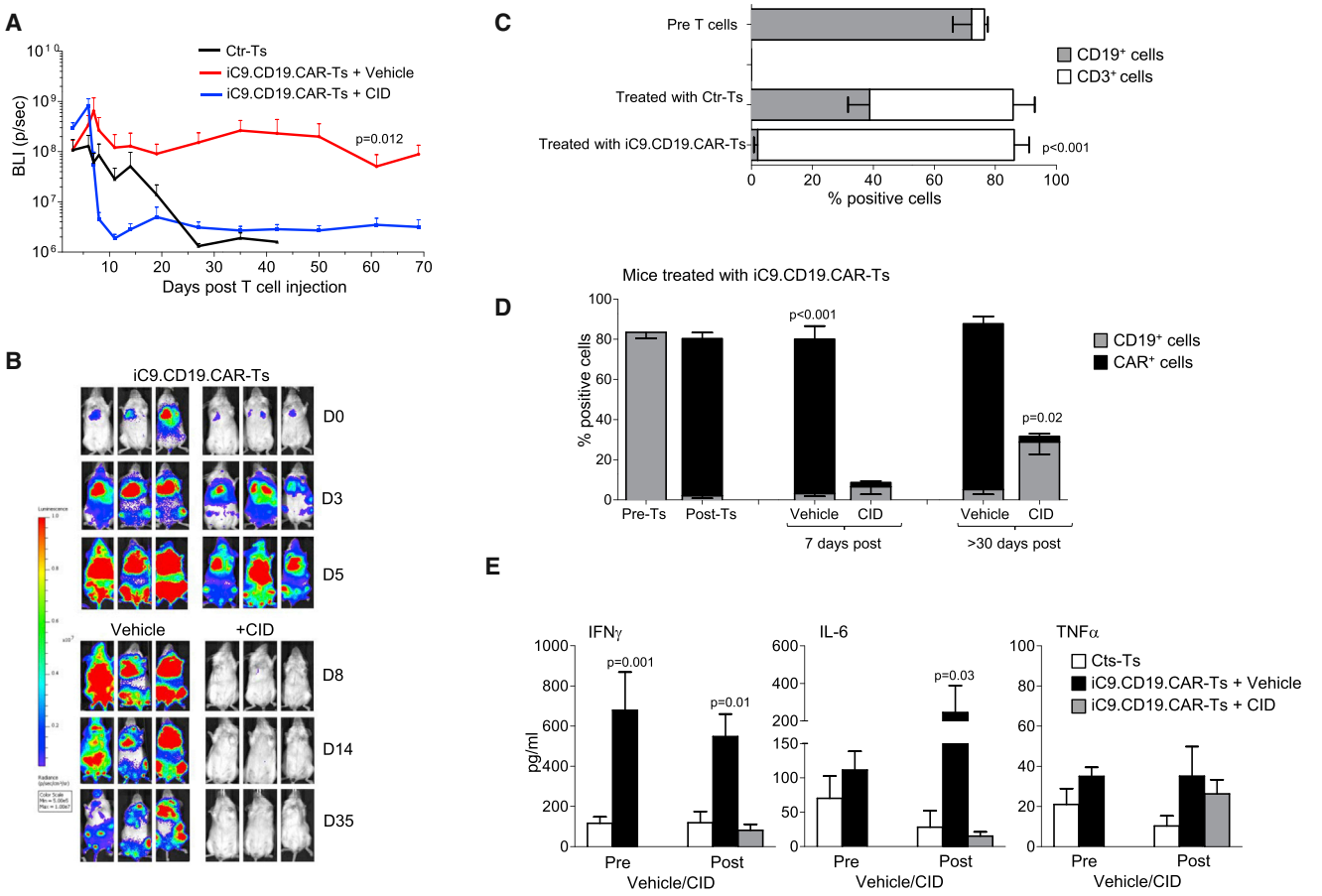


**Figure 3. In Vivo Expansion of iC9.CD19.CAR-Ts and Effects of CID**

NSG mice were engrafted with CD34$^+$ cells isolated from umbilical cord blood units and, upon engraftment of human hematopoietic cells, infused with Ctr-Ts or iC9.CD19.CAR-Ts labeled with eGFP-FFluc. (A) Summary of bioluminescence signals (BLI, total plux) of Ctr-Ts (13 mice) and iC9.CD19.CAR-Ts treated with either vehicle (16 mice) or CID (50 μg/mouse) (8 mice) by day 6. Lines are average (±SEM) of the bioluminescence intensity for each group. (B) Images from representative mice before and after receiving either vehicle or CID. (C) Percentage of circulating CD19$^+$ (gray bars) and CD3$^+$ (white bars) cells (gated on human CD45$^+$ cells) in mice before and after receiving Ctr-Ts or iC9.CD19.CAR-T cells. (D) Percentage of circulating CD19$^+$ (gray bars) and CAR$^+$ (black bars) cells (gated on human CD45$^+$ cells) in mice before (Pre-Ts) and after (Post-Ts) iC9.CD19.CAR-Ts infusion. Shown are also data before and after (7 or >30 days) treatment with vehicle or CID (50 μg/mouse). Bars are means ± SEM of at least ten mice/group. (E) IFN-γ, TNF-α, and IL-6 measured in the plasma of mice treated as per (C and D). Bars are means ± SEM.

### iC9.CD19.CAR-Ts Proliferate In Vivo in a Humanized Mouse Model but Are Efficiently Eliminated by CID, Allowing B Cell Reconstitution

To validate in vivo the activity of iC9.CD19.CAR-Ts, we used a humanized mouse model generated by engrafting CD34$^+$ cells in sub-lethally irradiated NSG mice.[21] Upon confirmed engraftment of human CD45$^+$ cells, mice received either Ctr-Ts or iC9.CD19.CAR-Ts, labeled with eGFP-FFLuc (Figure S2A). T cell expansion was monitored by bioluminescence intensity (BLI). Since the purpose of these experiments was to assess primarily the capacity of iC9 to control the toxic effects of iC9.CD19.CAR-Ts associated with CRS, we used allogeneic Ctr-Ts and iC9.CD19.CAR-Ts to maximize their in vivo expansion in response to the CD19 antigen expressed by B lymphocytes. For these experiments, we used iC9.CD19.CAR-Ts selected with 3 μL/10$^7$ cells of NGFR-PE Ab, which warranted acceptable T cell recovery and adequate response to CID. Our data were also confirmed in additional experiments with mice infused with Ctr-Ts and iC9.CD19.CAR-Ts not labeled with eGFP-FFLuc. Starting from day 2 post-infusion, iC9.CD19.CAR-Ts expanded rapidly and at significantly higher level as compared to Ctr-Ts (Figure 3A) or to iC9.CD19.CAR-Ts infused in non-humanized NSG mice (Figure S3B), confirming that the increase/expansion of iC9.CD19.CAR-Ts is predominantly mediated by the engagement of the CD19 expressed by B cells. The BLI increase was paralleled by a greater increment of circulating CD3$^+$ (and CAR$^+$) cells in mice infused with iC9.CD19.CAR-Ts (84% ± 2%) as compared to mice infused with Ctr-Ts (54% ± 7.5%; p = 0.003) (Figure 3C). Mice infused with iC9.CD19.CAR-Ts labeled with eGFP-FFluc were treated by day 7 post-T cell infusion, when the BLI usually reached the highest values, with either AP20187 (CID 50 μg/mouse) or AP20178 diluent (vehicle). BLI rapidly

decreased only in mice receiving CID and remained low over the following observation period ($p < 0.001$; Figures 3A and 3B). This was paralleled by the disappearance of iC9.CD19.CAR-Ts only in mice treated with CID (2.2% ± 0.6% versus 77% ± 6.5%; $p < 0.001$) (Figure 3D). All mice receiving Ctr-Ts maintained circulating $CD19^+$ B lymphocytes (38.8% ± 7.1% of the $CD45^+$ human cells), while mice infused with iC9.CD19.CAR-Ts almost completely cleared B lymphocytes post-T cell infusion (2% ± 1.3%; $p < 0.001$ by day 7 post-T cells) (Figure 3C). $CD19^+$ B cells started to recover in peripheral blood only in mice treated with CID (6.5% ± 3.7%, $p = 0.4$) (Figures 3D and S2C). B cell reconstitution and lack of iC9.CD19.CAR-Ts were observed long term in mice treated with CID (28.8% ± 6%; $p = 0.02$% and 2.9% ± 1.3%; $p < 0.001$%, respectively), while B cell aplasia and iC9.CD19.CAR-Ts persisted in mice that received vehicle (Figures 3D and S2D). When we analyzed the health conditions of the mice, we found that five of the 13 (38%) mice infused with Ctr-Ts developed signs consistent with xenograft versus host disease (GVHD), including fur and weight loss (18 ± 0.6 gr) and hunched posture, and these mice required euthanization within 30 days after T cell infusion. In contrast, none of the mice treated with iC9.CD19.CAR-Ts experienced significant loss weight (21 ± 0.5 gr, $p = 0.031$). Interestingly, mice receiving iC9.CD19. CAR-Ts experienced a transient weight loss (compared to pre CAR-T weight of 22.6 ± 0.4 gr, $p = 0.028$) and agitation within 10 days from T cell infusion. Although we did not monitore fever or blood pressure (all signs associated with CRS in humans),[22] we measured higher level of human cytokines like IFN-γ, IL-6, and tumor necrosis factor alpha (TNF-α) (Figure 3E) in the plasma of mice treated with iC9.CD19.CAR-Ts (compared to those treated with Ctr-Ts), which resemble the profile of cytokines released in sera of patients treated with CD19.CAR-Ts experiencing CRS.[2,23] Importantly, we observed that IL-6 (111 ± 27 pg/mL) decreased in mice treated with iC9.CD19.CAR-Ts once they received CID (to 15 ± 6 pg/mL; $p < 0.05$) but increased in mice receiving vehicle (to 245 ± 143 pg/mL; Figure 3E). Overall, only three of the 16 mice (19%) treated with iC9.CD19.CAR-Ts and receiving vehicle died of indeterminate causes (pathology was not available to distinguish between either GVHD or sustained pro-inflammatory conditions induced by the continuous expansion of iC9.CD19.CAR-Ts), while all mice treated with CID fully recovered including their body weight (21.7 ± 0.5 gr; p = not significant [NS]).

### iC9.CD19.CAR-Ts Have Antitumor Activity In Vivo

Having shown that iC9.CD19.CAR-Ts deplete normal B lymphocytes in our humanized mice, we used this model to test CD19.CAR-Ts antitumor activity. Humanized mice, upon confirmed engraftment of $CD45^+$ cells, received FFluc-labeled Daudi cells, and, 3 days later, Ctr-Ts or iC9.CD19.CAR-Ts.[5] When tumor growth was clearly detectable by an in vivo imaging system (IVIS) in the Ctr-Ts group, mice infused with iC9.CD19.CAR-Ts were randomized for vehicle or CID (50 μg/mouse) administration (Figure 4). While tumor-BLI rapidly increased in mice treated with Ctr-Ts, tumor signals remained low in mice infused with iC9.CD19.CAR-Ts regardless of whether they received vehicle or CID (Figure 4A). Normal B cells rapidly disappeared from the circulation after the infusion of iC9.CD19.CAR-Ts. $CD19^+$ B cells with λ- and κ-light restricted chains reconstituted in mice receiving CID, while remaining undetectable in mice infused with vehicle (Figure 4B). Mice infused with iC9.CD19.CAR-Ts showed no significant differences in tumor-free survival when treated with vehicle or CID. By day 80 post-infusion, tumor had developed in three of 24 (13%) mice receiving vehicle and in four of 18 mice (22%) receiving CID (Figure 4C). Late tumor recurrence especially in the CNS was observed, which is consistent with our previous results in non-humanized mouse models (data not shown).

### The Pro-apoptotic Function of the iC9 Can Be Modulated In Vitro

T cells expressing iC9 display in vitro a CID dose-response induction of apoptosis.[11,17] Similarly iC9.CD19.CAR-Ts retained a titratable induction of apoptosis in response to CID in vitro (Figure 5A). To demonstrate that the expression levels of iC9 are critical in defining the fraction of cells spared by exposure to low doses of CID, positively selected iC9.CD19.CAR-Ts were expanded ex vivo and then further flow-sorted in $NGFR^{low}$ and $NGFR^{high}$-expressing cells (Figure 5B). Sorted cells were then exposed to either 0.1 or 10 nM of CID. $NGFR^{high}$ cells were consistently <10% viable when incubated with either 0.1 or 10 nM of CID, while $NGFR^{low}$ cells were significantly spared when exposed to 0.1 nM of CID ($p < 0.05$; Figure 5C). We also found that the prominent dose effect of the CID in $NGFR^{low}$ cells was due to their activation status. Upon T cell receptor (TCR) activation, $NGFR^{low}$ cells showed similar susceptibility to apoptosis when exposed to 0.1 or 10 nM of CID (6.1% ± 3% versus 11.4% ± 3.5% viable cells) (Figures 5C and S3A) and increased transcription of the *iC9* transgene, since the copies of *iC9* per integration reached values equivalent to those of non-activated $NGFR^{high}$ cells (Figure 5D). Importantly, we confirmed that iC9.CD19.CAR-Ts spared after incubation with 0.1 nM of CID retained functional expression of the CAR (Figure S3B), as indicated by their capacity to lyse $CD19^+$ tumor cells in short term (Figures 5E and 5F) and long-term killing assays (Figure S3E). We have also performed immunophenotypic analyses to determine memory and exhaustion markers in T cells spared after exposure to low doses of CID. Overall, the only significant difference was observed in the frequency of $Tim3^+$ cells (from 58% ± 9.5% to 25% ± 3.4%, $p = 0.0053$), but not in other exhaustion markers like PD1 or CD57 (Figures S3C and S3D). We observed a slight but not significant reduction in $CD8^+$, $CD45RA^+CCR7^+$, and $CD27^+CD28^+$ cells (Figures S3C and S3D), which express the CAR/NGFR molecules at modestly brighter levels. Finally, iC9.CD19.CAR-Ts spared upon exposure to low doses of CID were infused into tumor-bearing mice and showed retained ability to control tumor growth (Figure S3F). Overall our data suggest that the exposure of iC9.CD19.CAR-Ts to CID does not cause selection of CAR-Ts phenotypically distinct from those eliminated by CID, and that CID-spared iC9.CD19.CAR-Ts maintain proliferative capacity and antitumor activity.

### The Viability of iC9.CD19.CAR-Ts Can Be Pharmacologically Modulated In Vivo by Titrating the Dose of the NGFR-PE Ab Used for Selection and the Dose of the CID

We then determined whether the pro-apoptotic function of iC9 can be modulated in vivo to contain the release of cytokines associated

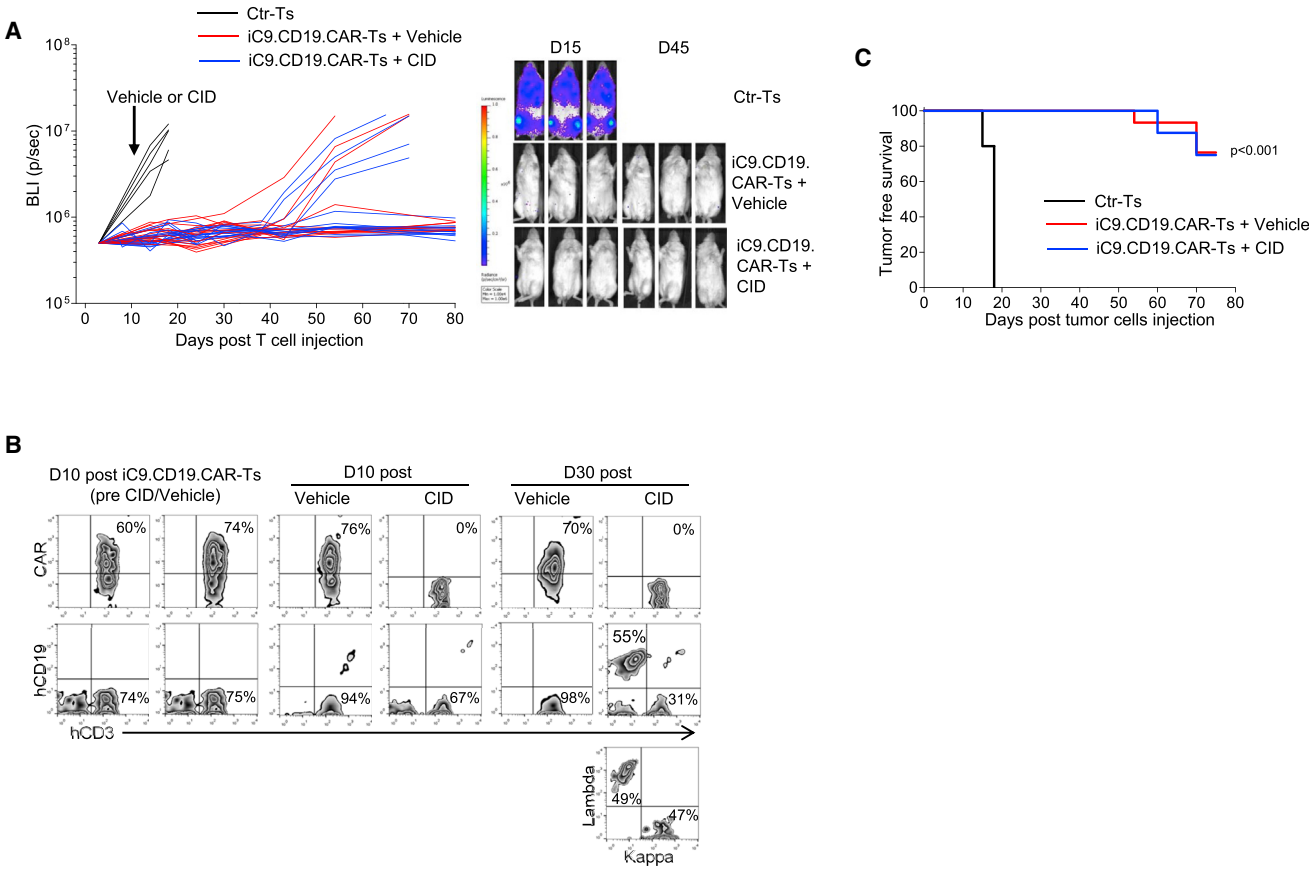


**Figure 4. In Vivo Antitumor Activity of iC9.CD19.CAR-Ts**

Upon engraftment of human hematopoietic cells, mice were infused with CD19$^+$ Daudi cells labeled with eGFP-FFluc. Three days later, mice received Ctr-Ts or iC9.CD19.CAR-Ts and 10 days later either vehicle or CID 50 μg/mouse. (A) Bioluminescence signals of the CD19$^+$ FFluc-Daudi tumor cells. The left panel shows the mean bioluminescence intensity (BLI) for each mouse/group, while the right panel illustrates images from three representative mice/group. (B) Immunophenotypic analyses of peripheral blood samples of representative treated mice at the indicated time point. Light-chain immunoglobulin restriction was analyzed long term on mice reconstituting normal CD19$^+$ B lymphocytes. (C) Shown is the Kaplan-Meier survival curve.

with CRS, without completely depleting iC9.CD19.CAR-Ts. We took advantage of our humanized mouse model and compared in mice the effects of iC9.CD19.CAR-Ts selected with stringent or less stringent NGFR-PE Ab-selection conditions, and different doses of CID. In the first set of experiments, eGFP-FFluc-labeled iC9.CD19.CAR-Ts selected using stringent conditions (3 μL/$10^7$ cells of NGFR-PE Ab) were infused in CD34$^+$ engrafted mice. Mice were then randomized, based on BLI, to receive either vehicle or decreasing doses of CID (50, 25, or 12.5 μg/mouse). While increasing in mice receiving vehicle, BLI decreased >2 logs within 24 hr after CID administration ($p < 0.02$), regardless of the dose (Figure 6A). Plasma levels of human IFN-γ, IL-6, and TNF-α were also equally reduced after CID administration, at all tested doses (Figure 6B). In sharp contrast, when iC9.CD19.CAR-Ts were selected using less stringent conditions of NGFR-PE Ab (6 μL/$10^7$ cells), we observed a CID dose-dependent elimination of iC9.CD19.CAR-Ts in vivo. Indeed, in mice treated with 12.5 μg/mouse of CID we discovered an inferior elimination of iC9.CD19.CAR-Ts compared to mice receiving higher CID doses ($p < 0.02$) (Figure 6C). Importantly, mice treated with iC9.CD19.CAR-Ts selected with less stringent conditions, and 12.5 μg/mouse of CID continued to produce significant amount of IFN-γ, while circulating levels of IL-6 were equally reduced as in mice treated with higher doses of CID (Figure 6D). In line with the inferior elimination of iC9.CD19.CAR-Ts after administration of a low dose of CID, these mice had reduced CD19$^+$ B cell recovery ($p < 0.05$; Figure 6E) and higher number of circulating iC9.CD19.CAR-Ts over time ($p < 0.05$; Figure 6F), as compared to mice receiving iC9.CD19.CAR-Ts selected with stringent conditions, where elimination of iC9.CD19.CAR-Ts allowed B cell recovery.

In selected experiments, Ctr-Ts or iC9.CD19.CAR-Ts were injected in mice with high FFluc-tumor burden (day 7 or 14 post-tumor inoculation). As observed in the experiments in which mice were treated in condition of low tumor burden, iC9.CD19.CAR-Ts still appropriately controlled tumor growth (Figures 7A and S4A). Mice were then divided in two groups and received vehicle or CID (12.5 μg/mouse)

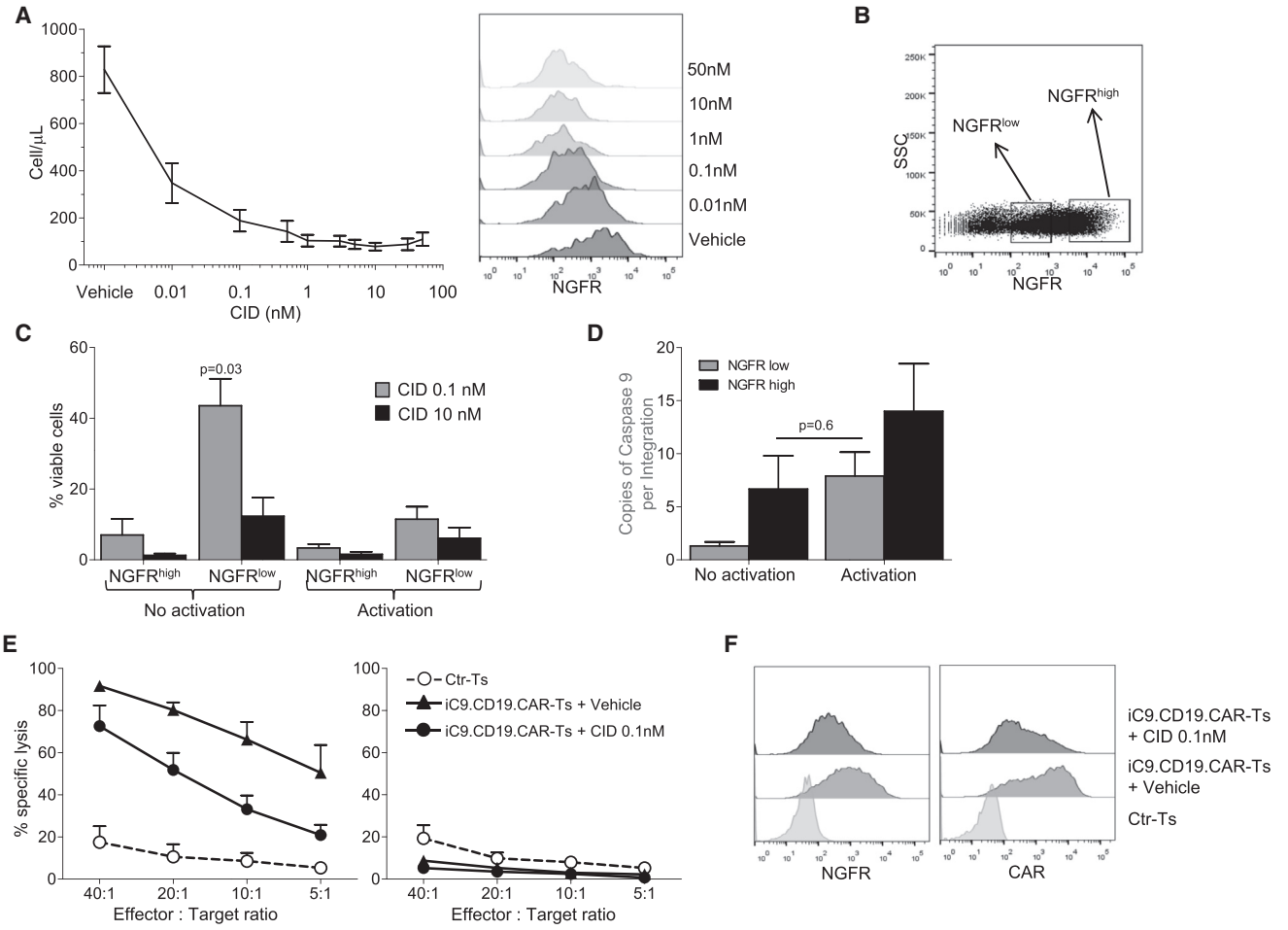


**Figure 5. Modulation of iC9.CD19.CAR-T Function In Vitro by CID**

(A) Number of viable iC9.CD19.CAR-Ts enumerated 24 hr after exposure to escalating doses of CID in vitro. Shown are mean ± SEM of T cell lines generated from seven healthy individuals. The histogram on the right shows the levels of NGFR expression in cells detected 24 hr after the exposure to the indicated doses of CID. (B) Shown is the cell-sorting gating strategy to isolate NGFR$^{high}$ and NGFR$^{low}$ iC9.CD19.CAR-Ts in one representative donor. (C) Percentage of viable iC9.CD19.CAR-Ts in NGFR$^{high}$ and NGFR$^{low}$-selected cells after the exposure to either 0.1 or 10 nM of CID and normalized to cells treated with vehicle. The experiment was repeated using iC9.CD19.CAR-Ts non-activated or activated with CD3/CD28 mAbs. (D) Copies of *iC9* transcripts/integration site in NGFR$^{high}$ and NGFR$^{low}$ cells non-activated or activated with CD3/CD28 mAbs. (E) Cytotoxic activity of iC9.CD19.CAR-Ts non-exposed to CID or exposed to 0.1 nM of CID. The left and right graphs show the percentage of lysis of the CD19$^{+}$ Raji and the CD19$^{-}$ HDLM-2 tumor cell lines, respectively, in a $^{51}$Cr-based release assay. Ctr-Ts were used as control. (F) Shown is the histogram of NGFR and CAR expression of the cells assayed for the cytotoxic activity in (E). Data are means ± SEM of T cell lines generated from four healthy individuals.

7–10 days post-T cell infusion as soon as the tumor BLI signal reached background levels. As shown in Figure 7A, mice remained tumor free by day 80 post-treatment. In parallel experiments, 5–10 days after the administration of CID (12.5 µg/mouse), mice were re-challenged with FFluc-tumor cells. Remarkably, iC9.CD19.CAR-Ts remaining after the administration of low doses of CID controlled tumor growth, unlike control mice (Figures 7B and S4B). This effect was clearly mediated by iC9.CD19.CAR-Ts that, spared by the administration of a low dose of CID, promptly re-expanded upon tumor re-challenge (Figure 7C). As shown in Figure 7D, tumor-free survival of mice treated with iC9.CD19.CAR-Ts and a low dose of CID was similar to that of mice receiving iC9.CD19.CAR-Ts and vehicle confirming the safety and efficacy of our proposed strategy.

## DISCUSSION

We have shown that the expansion of CD19.CAR-Ts can be tightly modulated when the vector encoding the CAR contains the iC9 safety switch and a selectable marker. The appropriate combination of stringency for the in vitro selection of iC9.CD19.CAR-Ts and the low doses of CID that activates the iC9 provides a specific containment of iC9.CD19.CAR-T expansion and cytokine release, without abrogating their function. When required, a higher dose of the CID can be used to completely eliminate iC9.CD19.CAR-Ts and promote the reconstitution of normal B lymphocytes.

While the administration of CD19.CAR-Ts has reached excellent response rates in B cell-derived malignancies, the associated toxicities

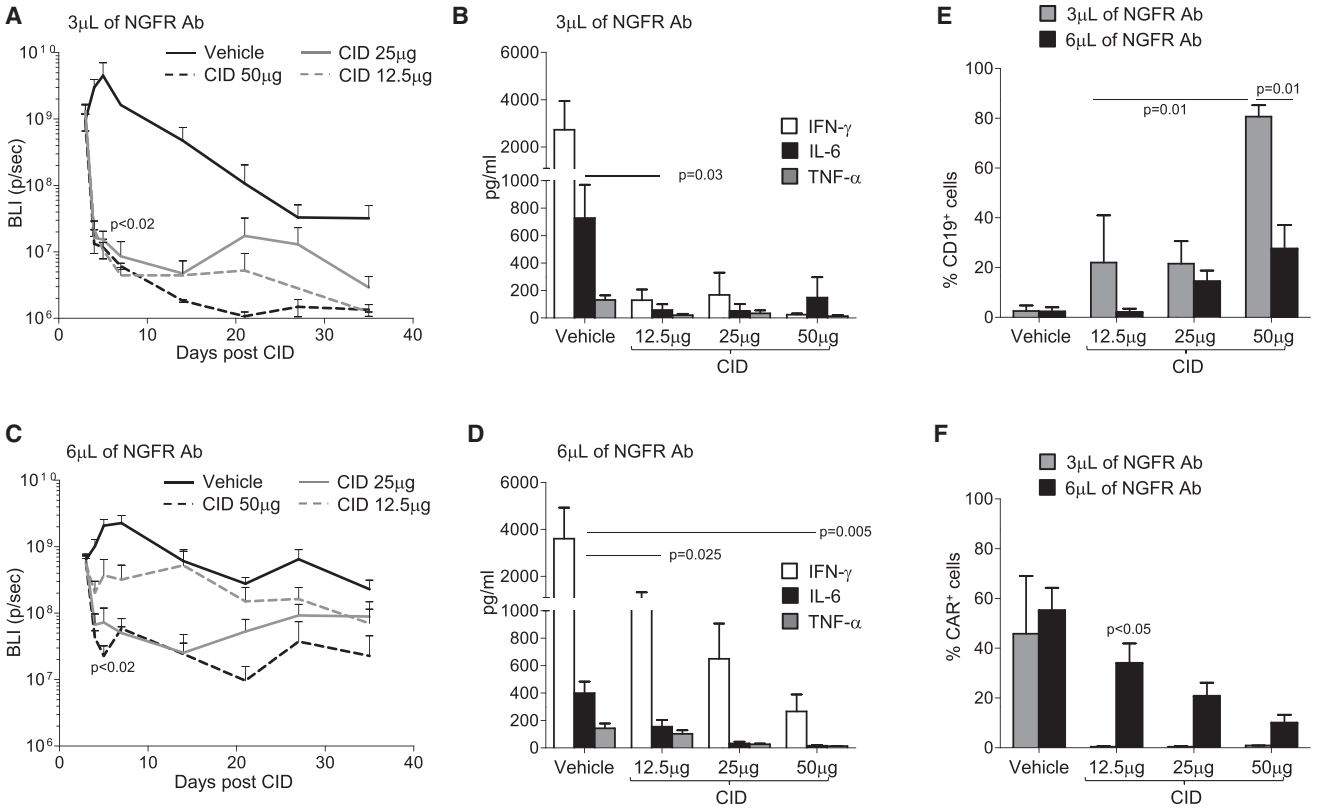


**Figure 6. Modulation of iC9.CD19.CAR-T Function In Vivo by CID**

Mice were infused with eGFP-FFLUc-iC9.CD19.CAR-Ts and treated at the peak of expansion with either vehicle or different doses of CID (50, 25, and 12.5 μg/mouse). For these experiments, iC9.CD19.CAR-Ts were selected using either 3 μL/$10^7$ cells (A and B) or 6 μL/$10^7$ cells (C and D) of the NGFR-PE Ab. (A) and (C) show bioluminescence signals (BLI) of iC9.CD19.CAR-Ts in mice treated with either vehicle or the indicated doses of CID. Lines show the means bioluminescence ± SEM for ten mice/group. (B) and (D) show the measurement of IFN-γ, IL-6, and TNF-α in the plasma of mice treated with iC9.CD19.CAR-Ts and analyzed 7 days after they received either vehicle or CID. Bars are means ± SEM of ten mice. (E) Percentage of circulating B cells in mice treated with iC9.CD19.CAR-Ts (selected with 3 μL/$10^7$ cells or 6 μL/$10^7$ cells of NGFR Ab) at days 35–40 after infusion of vehicle or CID. Bars are means ± SEM of ten mice. (F) Percentage of circulating iC9.CD19.CAR-Ts (selected with 3 μL/$10^7$ cells or 6 μL/$10^7$ cells of NGFR Ab) at days 35–40 after infusion of vehicle or CID. Bars are means ± SEM of ten mice.

require further refinement for this strategy. B cell aplasia is an indicator of CD19.CAR-T persistence and function.[2] Given that the number of patients infused with CD19.CAR-Ts is rapidly increasing, it will be soon possible to correlate sustained clinical responses with the duration of the B cell aplasia and likely define a therapeutic window in which it is reasonably safe to terminate the effects of CD19.CAR-Ts without causing tumor relapse. Thus, on-demand blunting of CD19.CAR-Ts to revert an undesired and unnecessary long-term B cell aplasia is a critical requirement. While T lymphocytes can be eliminated by lymphodepleting chemotherapy, antibodies, or high-dose steroids, the incorporation of a safety switch within CAR-Ts represents a more precise and selective approach. Safety switches encoded in combination with CARs include the iC9, herpes simplex thymidine kinase (*HSV-TK*), epidermal growth factor receptor (EGFR), and CD20, which induce T cell death upon exposure to CID, ganciclovir, cetuximab, and rituximab, respectively.[5,7,8,25,26] All these safety switches seem equally effective in eliminating the transduced T cells, but only iC9, and HSV-TK have been extensively tested clinically, in the context of the donor leucocyte infusion after haploidentical stem cell transplant.[12–14,27,28] Of these two options, iC9 may have a superior clinical profile, when taking into account the selectivity and rapidity of T cell elimination and the low level of immunogenicity.[29]

The iC9 has been used in the past to efficiently eliminate CAR-Ts preclinically in the context of immuno-deficient mice, but its function and specifically its tuning properties have never been tested in a humanized mouse model. We have demonstrated here that when the iC9 safety switch is combined with the CD19.CAR, iC9.CD19.CAR-Ts can be efficiently eliminated by the administration of CID, allowing the reconstitution of normal B lymphocytes. In addition, although with the limits of a mouse model, we show that the ablation of iC9.CD19.CAR-Ts after the elimination of the tumor cells does not necessarily cause tumor relapse. Although it has been reported that adoptive transfer of human T or CAR-Ts in NSG mice can lead to the development of xeno-GVHD[30] and a fraction of our

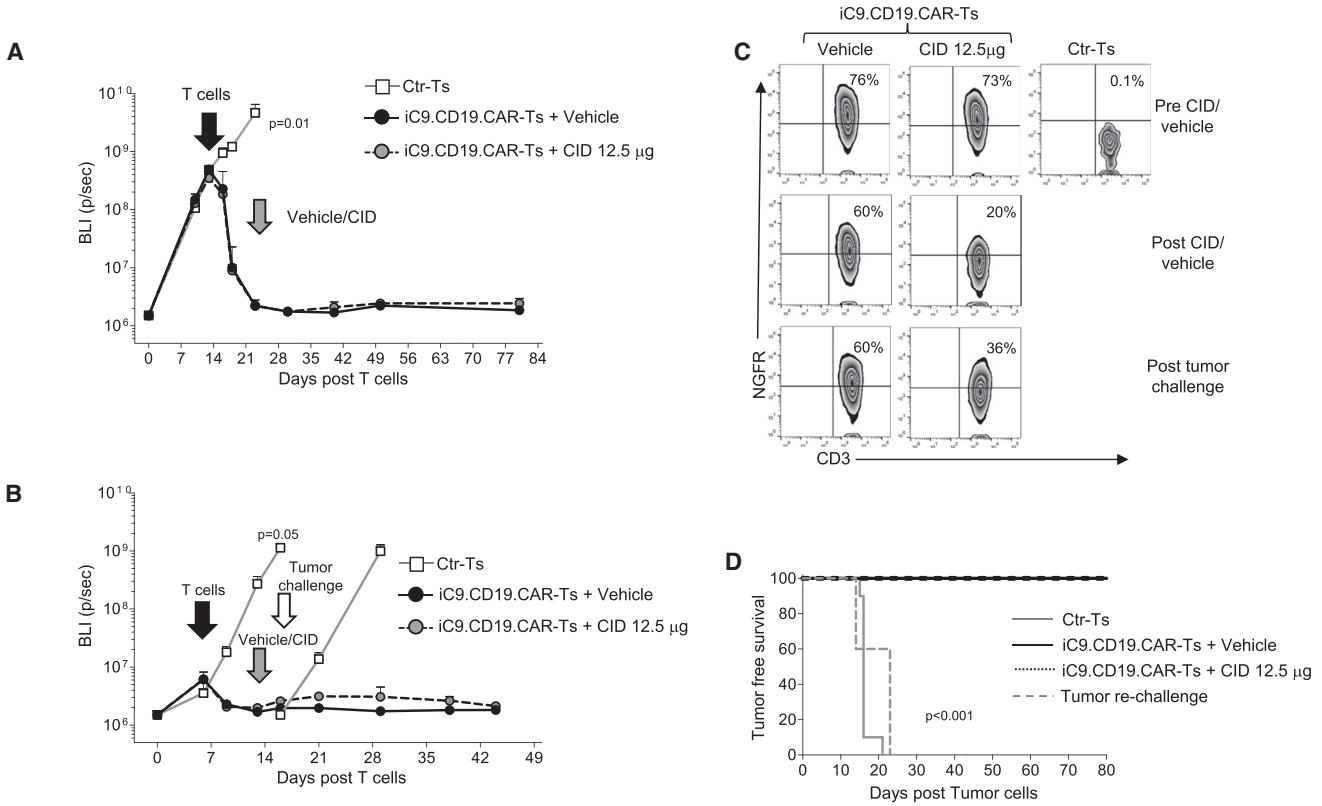


**Figure 7. Modulation of iC9.CD19.CAR-T Function In Vivo in High Tumor Burden and Re-challenge Tumor Models**

FFLUc-tumor engrafted mice received Ctr-Ts or iC9.CD19.CAR-Ts on days 14 (A) or 10 (B) (ten mice/group). (A) Upon decrease of tumor bioluminescence signals after iC9.CD19.CAR-T treatment, mice were randomized to receive either vehicle or CID (12.5 μg/mouse) and monitored over time for tumor growth. (B) In selected experiments, 5 days post-vehicle or CID treatment (12.5 μg/mouse), mice were re-challenged with the same dose of FFluc-CD19$^+$ tumor cells and monitored over time for tumor growth. (C) Immunophenotypic analyses of peripheral blood samples of representative mice treated according to the schedule described in (B). (D) Kaplan-Meier survival curve of combined experiments in (A) and (B). Data are means ± SEM of ten mice.

control mice develop symptoms compatible with GVHD, our data suggest that the CAR-driven effect (B cell aplasia and antitumor activity) can be differentiated from any potential allogeneic/xenogeneic effects, as no apparent symptoms compatible with GVHD occurred in our CAR-Ts-treated mice, while no B cell aplasia or control of tumor growth occurred in control mice. Our observed results are not surprising as, in a previously reported immunocompetent murine model, GVHD occurring in mice receiving allogeneic CD19.CAR-Ts was mediated exclusively by CD4$^+$ CAR-Ts and importantly only when CAR-Ts were given 2 days after bone marrow transplant conditioning therapy.[24] Our model has no conditioning that would exacerbate GVHD and is also in line with the robust clinical evidences from National Cancer Institute in which donor-derived CD19.CAR-Ts infused in the context of allogeneic stem cell transplant (without prior chemotherapy or conditioning, as in our model) do not cause GVHD, suggesting that the CAR-mediated signaling may overcome the TCR-mediated signaling.[31]

The control of the CRS, which is another critical side effect of CD19.CAR-Ts, is matter of intense investigation. CRS development correlates with the expansion of CD19.CAR-Ts and its clinical manifestations are largely associated with high plasma levels of IL-6.[1,2,22,23] The administration of Tocilizumab, which blocks the IL-6 receptor and effectively controls the clinical manifestations of CRS, and algorithms have been developed in the attempt to define the optimal time for the administration of Tocilizumab to control life-threatening CRS, without dramatically diminishing the antitumor effects of CD19.CAR-Ts.[2,22,23] However, a more precise control of CD19.CAR-T expansion seems desirable. Elegant approaches have been proposed to regulate the expansion of CAR-Ts by pharmacologically controlling T cell co-stimulation.[32] Here, we suggest that the iC9 safety switch not only can be used to terminate the effects of iC9.CD19.CAR-Ts, but also can modulate their apoptotic rate, thus controlling their expansion and the concomitant cytokine load.

The humanized mouse model we propose seems to mirror the role of IL-6 as a player in the CRS clinical picture. Recent evidences point out at IL-6 being produced by myeloid cells in response to the activated T cells,[24] and, while the mechanism is still under investigation, our model for the first time attempts to recapitulate these events. In this

model, we show indeed that the iC9 safety switch has the unique property to tune the expansion of iC9.CD19.CAR-Ts and reduce the levels of circulating IL-6 when low doses of CID are used. Nonetheless, iC9.CD19.CAR-Ts spared by low doses of CID remain effective in controlling tumor growth.

Experiments in vitro showed that 10–20 nM of CID are generally sufficient in inducing >90% apoptosis of iC9-engineered T cells.[11] The administration of 0.4 mg/kg of CID causes over 85%–90% elimination of iC9-engineered T cells in vivo.[12,14] Of note, iC9-engineered T cells not responding to the CID in vivo are not intrinsically resistant to the drug but rather show either lower copy numbers of the transgene, or relatively low transcriptional activity, resulting in lower iC9 protein expression and thus reduced susceptibility to apoptosis CID mediated.[33] Taking advantage of this observation, we now proved that, while high doses of CID remove most of the iC9.CD19.CAR-Ts, lower doses preferentially eliminate iC9.CD19.CAR-Ts characterized by either multiple copies of the transgene or higher transcriptional activity, sparing cells with lower copy numbers or low transcriptional activity. We confirmed that the iC9.CD19.CAR-Ts spared by low doses of CID retain CD19.CAR functionality in vitro and can be effectively eliminated upon activation that mediates increased transcriptional activity. More importantly, we demonstrated in the humanized mouse model that low doses of CID calibrate the expansion of iC9.CD19.CAR-Ts at sufficient levels to control plasma levels of IL-6, while maintaining tumor control and protecting from tumor re-challenge. Of note, we also showed that the inclusion of the truncated form of the NGFR receptor as a selectable marker plays a decisive role. Taking in consideration the variability in transduction efficiency of iC9.CD19.CAR-Ts and the threshold levels of iC9 expression in causing T cell apoptosis after exposure to CID, the selection of transduced cells based on the expression of the truncated form of NGFR ensures a more consistent and predictable pattern of transgene expression.

In summary, we showed that the iC9 safety switch incorporated within the CD19.CAR provides the opportunity for balancing expansion/toxicity and persistence/protection of CD19.CAR-Ts ensuring their modulation in case of toxicities, like CRS, or their complete ablation to restore B cell immunity. Although, the dimerizer drug is not licensed for clinical indication, we are implementing a phase I clinical study in collaboration with Bellicum Pharmaceutical aimed at identifying the lowest dose of AP1903 allowing control of severe CRS without ablating iC9.CD19.CAR-Ts to validate our observations in patients.

## MATERIALS AND METHODS

### Cell Lines

293T cells, Daudi and Raji ($CD19^+$ Burkitt lymphoma cell lines), K562, and HDLM-2 ($CD19^-$ tumor cell lines) were purchased from the American Type Culture Collection (ATCC) or the German Collection of Microorganisms and Cell Cultures GmbH (DSMZ) and maintained in culture with RPMI-1640 (Gibco-BRL) supplemented with 10% fetal bovine serum (FBS-HyClone, GE Healthcare) and 2 mM GlutaMAX (Gibco-BRL) in a humidified atmosphere containing 5% $CO_2$ at 37°C. In selected in vivo experiments, Daudi cells were transduced with a retroviral vector encoding the Firefly-Luciferase gene (*FFLuc*).[34] Cell lines were authenticated by the University of Texas MD Anderson Cancer Center Characterized Cell Line Core Facility (Houston, TX). All lines were routinely checked over the course of the experiments and always found mycoplasma free and routinely validated by flow cytometry for surface markers and functional readouts as needed.

### Generation of Retroviral Supernatant

We generated two retroviral vectors using the SFG backbone encoding either CD19-specific CAR alone (CD19.CAR)[35] or three genes (*iC9*,[11] a truncated form of the human low-affinity nerve growth factor receptor, ΔNGFR,[19] and the CD19.CAR)[35] (iC9.CD19.CAR) linked by two 2A-like sequences (Figure 1A).[5,36] The CD19.CAR contains the 4-1BB co-stimulatory endodomain.[37] For T cells, we generated a retroviral vector encoding the eGFP-Firefly-Luciferase (*eGFP-FFluc*) gene.[36] The cassettes cloned into the vectors were sequenced. Transient retroviral supernatants were produced by transfection of 293T cells with the RD114 envelope (RDF plasmid), the MoMLV gag-pol (PegPam3-e plasmid), and the retroviral vector.[34]

### T Cell Transduction and Expansion

Buffy coats from healthy donors were obtained through the Gulf Coast Regional Blood Center, Houston, TX. Peripheral blood mononuclear cells (PBMCs), isolated with Ficoll-Paque (Amersham Biosciences, GE Healthcare), were activated using immobilized OKT3 or anti-CD3 (Miltenyi Biotec) and CD28 (BD Biosciences) antibodies (Abs). On day 3, cells were transduced with retroviral supernatants and expanded in complete medium (45% RPMI-1640 and 45% Click's medium [Irvine Scientific], 10% FBS, and 2 mM GlutaMAX) and with interleukin-7 (IL-7) (10 ng/mL; PeproTech) and IL-15 (5 ng/mL; PeproTech), every 2–3 days.[38] On day 8, cells were positively selected using the CD271 Microbeads Kit (Miltenyi Biotec) consisting of NGFR-PE and anti-PE beads. After selection, cells were plated in complete medium with IL-7 and IL-15 for up to 18 days.[38,39] In parallel, we expanded in IL-7 and IL-15 mock-transduced (empty SFG) T cells (Ctr-Ts). In selected experiments, both Ctr-Ts and iC9.CD19.CAR Ts were transduced with a retroviral vector encoding *eGFP-FFLuc* the day after transduction with the first vector.[5]

### Flow Cytometry

Monoclonal Abs for CD45, CD3, CD8, CD19, CD20, CD45RA, CD45RO, CD28, CD95, CD62L, CD14, CD33, κ/λ-light chains, and CD271 (BD Biosciences) and CCR7 (R&D Systems) were used. Expression of the CD19.CAR was detected using a specific anti-idiotype scFv monoclonal antibody (mAb) (kindly provided by Dr. Lawrence Cooper, MD Anderson Cancer Center).[40] Cells were collected using a BD-FACSCalibur, a five-laser BD-Fortessa, or the Gallios Flow Cytometer (Beckman Coulter) and analyzed using FlowJo software v.9.3 (Tree Star) or Kalusa software. In selected experiments, counting beads (CountBright, Invitrogen) were added following manufacturer's instruction.

### Short-Term Cytotoxic Activity

The cytotoxic activity of T cells against $CD19^+$ and $CD19^-$ tumor cells was determined using a standard 4-hr $^{51}Cr$-release assay at different effector-to-target ratios (E:T; 40:1, 20:1, 10:1, and 5:1) and using a γcounter (Perkin-Elmer).[34]

### Long-Term Cytotoxic Activity

Tumor cells were seeded in 24-well plates at a concentration of $5 \times 10^4$/well. T cells were added to the culture at different ratios (E:T of 5:1; 1:1, or 1:3) without cytokines. Supernatant was collected after 24 hr to measure cytokine release and cells analyzed by day 5 to measure residual tumor cells and T cells by fluorescence-activated cell sorting (FACS) analysis based on CD20 and CD3 expression, respectively.[5,34]

### Proliferation Assay

T cells were labeled with 1.5 mmol/L carboxyfluorescein diacetate succinimidyl ester (CFSE; Invitrogen) and plated with irradiated tumor targets at an E:T ratio of 1:1. CFSE dilution was measured on $CD3^+$ cells by flow cytometry.[5]

### Activation of the Safety Switch

The B/B homodimerizer AP20187, a caspase inducible drug (CID) (Clontech Laboratories), was added at various concentrations to T cell cultures and induction of apoptosis evaluated 24 hr later using Annexin-V/7-AAD staining (BD Biosciences) and FACS analysis. In selected experiments, AP20187 was added to cells (non-activated or 24 hr after activation with immobilized CD3 and CD28 mAbs) for 3–4 hr. Cells were subsequently washed, re-plated to mimic the rapid clearance of the drug after in vivo administration,[12,41] and then counted based on viability using CountBright beads, to assess residual cytotoxic activity and NGFR expression. Extensive immune-phenotypic analyses were also performed, using the same panel of antibodies described in the flow cytometry section.

### Sorting of $NGFR^{high}$ versus $NGFR^{low}$ T Cells

In five donors, iC9.CD19.CAR-Ts were labeled with NGFR-PE and sorted in $NGFR^{low}$ (MFI mean: 494 ± 31) versus $NGFR^{high}$ (MFI mean: 9,097 ± 1,085)-expressing cells using the Flow Sorting Core at the University of North Carolina (Chapel Hill, NC). Sorted cells were tested to determine the expression of *iC9* per integration copies.[33]

### Measurement of Cytokines

Supernatants from T cell cultures and plasma from mice were analyzed for cytokines using the Th17-specific Milliplex assay kit (Millipore) following manufacturer's instructions. Data were analyzed using the Lumina-200 System and analyzed using the Milliplex Analyst 5.1 software (Millipore).

### Humanized Mouse Models to Assess Expansion and Antitumor Activity of T Cells

De-identified umbilical cord blood units (UCBs) were obtained through the MD Anderson Cord Blood Bank (University of Texas, Houston, TX) on a Baylor College of Medicine (BCM) institutional review board (IRB)-approved protocol or from the Carolinas Cord Blood Bank (Duke Translational Research Institute, Durham, NC) on a UNC-IRB-approved protocol. $CD34^+$ cells were isolated using immunomagnetic beads (Miltenyi) according to manufacturer's instructions. In vivo experiments were performed according to BCM's Animal Husbandry guidelines on a BCM institutional animal care and use committee (IACUC)-approved protocol and according to UNC's Animal Husbandry guidelines on a UNC-IACUC approved protocol. Four-week-old female NSG mice (Jackson Laboratory and UNC Animal Studies Core Facility) received intravenously (i.v.) $2 \times 10^5$ $CD34^+$ cells after sub-lethal irradiation (250 rad). After 4–6 weeks, mice were analyzed for the engraftment of human-derived $CD45^+$ cells, including lymphocytes and myeloid cells[21] and then infused with either $5 \times 10^6$ Ctr-Ts or iC9.CD19.CAR-Ts, labeled with FFluc to monitor proliferation and persistence using the Xenogen-IVIS Imaging System (Caliper Life Sciences).[5] To assess the function of the iC9, mice were infused intraperitoneally (i.p.) with different doses of AP20187. T cell bioluminescent signal intensity (BLI) was measured as total photon/s/$cm^2$/sr (p/s/$cm^2$/sr).[5,36] To assess functional activity of T cells, mice were bled at specific intervals (10–15 days, as per BCM- and UNC-IACUC guidelines) to assess plasma cytokines and frequency of $CD19^+$ and $CD3^+$ cells. The percentage of positive cells was calculated based on human $CD45^+$-gated cells. To assess antitumor activity, mice received $2 \times 10^6$ FFluc-labeled Daudi cells[5] and either Ctr-Ts or iC9.CD19.CAR-Ts or in selected experiments ex vivo-CID pretreated iC9.CD19.CAR-Ts. Tumor growth was measured by Xenogen-IVIS Imaging System. Mice were followed for up to 90 days. Blood, spleen, bone marrow, and spinal cord cells were collected and analyzed to detect the presence of human $CD45^+$, $CD19^+$, and $CD3^+$ cells and iC9.CD19.CAR-Ts. In selected experiments, mice received T cells only when BLI signal indicated high tumor burden. As soon as BLI declined indicating tumor elimination, mice were randomized to receive vehicle or CID (12.5 μg/mouse) and then monitored for tumor recurrence. In selected experiments, 7 days after CID treatment, mice were re-challenged i.v. with $2 \times 10^6$ FFluc-labeled Daudi cells and then monitored for tumor growth.

### Statistical Analysis

All in vitro data are presented as average ± SEM. The statistical significance of results with multiple comparisons was evaluated by repeated-measures ANOVA. Student's t test was used to determine the statistical significance of differences between samples, and $p < 0.05$ was accepted as indicating a significant difference. For the BLI experiments, intensity signals were summarized using average ± SEM at baseline and multiple subsequent time points for each group of mice. Changes in intensity of signal from baseline at each time point were calculated and compared using paired t tests or Wilcoxon signed-rank test. Survival curves were generated by GraphPad Prism v.5.0 for Mac (GraphPad).

## SUPPLEMENTAL INFORMATION

Supplemental Information includes four figures and can be found with this article online at http://dx.doi.org/10.1016/j.ymthe.2017.01.011.

## AUTHOR CONTRIBUTIONS

I.D., G.D., and B.S. designed the research, analyzed the data, and wrote the manuscript; M.Z., B.B., Y.C., and J.W. performed some of the experiments. All authors approved the final version of the manuscript.

## CONFLICTS OF INTEREST

The authors declare no conflict of interest.

## ACKNOWLEDGMENTS

This work was supported in part by a SCOR grant from the Leukemia and Lymphoma Society and Tier 2-Stimulus Award, Lineberger Comprehensive Cancer Center, University of North Carolina. The authors would like to thank Thomas Anthony Curtis and Brandon Kale (UNC, Chapel Hill, NC) for technical support with some experiments.

## REFERENCES

1. Lee, D.W., Kochenderfer, J.N., Stetler-Stevenson, M., Cui, Y.K., Delbrook, C., Feldman, S.A., Fry, T.J., Orentas, R., Sabatino, M., Shah, N.N., et al. (2015). T cells expressing CD19 chimeric antigen receptors for acute lymphoblastic leukaemia in children and young adults: A phase 1 dose-escalation trial. Lancet *385*, 517–528.
2. Maude, S.L., Teachey, D.T., Porter, D.L., and Grupp, S.A. (2015). CD19-targeted chimeric antigen receptor T-cell therapy for acute lymphoblastic leukemia. Blood *125*, 4017–4023.
3. Brentjens, R.J., Davila, M.L., Riviere, I., Park, J., Wang, X., Cowell, L.G., Bartido, S., Stefanski, J., Taylor, C., Olszewska, M., et al. (2013). CD19-targeted T cells rapidly induce molecular remissions in adults with chemotherapy-refractory acute lymphoblastic leukemia. Sci. Transl. Med. *5*, 177ra38.
4. Kochenderfer, J.N., Dudley, M.E., Kassim, S.H., Somerville, R.P., Carpenter, R.O., Stetler-Stevenson, M., Yang, J.C., Phan, G.Q., Hughes, M.S., Sherry, R.M., et al. (2015). Chemotherapy-refractory diffuse large B-cell lymphoma and indolent B-cell malignancies can be effectively treated with autologous T cells expressing an anti-CD19 chimeric antigen receptor. J. Clin. Oncol. *33*, 540–549.
5. Hoyos, V., Savoldo, B., Quintarelli, C., Mahendravada, A., Zhang, M., Vera, J., Heslop, H.E., Rooney, C.M., Brenner, M.K., and Dotti, G. (2010). Engineering CD19-specific T lymphocytes with interleukin-15 and a suicide gene to enhance their anti-lymphoma/leukemia effects and safety. Leukemia *24*, 1160–1170.
6. Wang, X., Chang, W.C., Wong, C.W., Colcher, D., Sherman, M., Ostberg, J.R., Forman, S.J., Riddell, S.R., and Jensen, M.C. (2011). A transgene-encoded cell surface polypeptide for selection, in vivo tracking, and ablation of engineered cells. Blood *118*, 1255–1263.
7. Casucci, M., Nicolis di Robilant, B., Falcone, L., Camisa, B., Norelli, M., Genovese, P., Gentner, B., Gullotta, F., Ponzoni, M., Bernardi, M., et al. (2013). CD44v6-targeted T cells mediate potent antitumor effects against acute myeloid leukemia and multiple myeloma. Blood *122*, 3461–3472.
8. Philip, B., Kokalaki, E., Mekkaoui, L., Thomas, S., Straathof, K., Flutter, B., Marin, V., Marafioti, T., Chakraverty, R., Linch, D., et al. (2014). A highly compact epitope-based marker/suicide gene for easier and safer T-cell therapy. Blood *124*, 1277–1287.
9. Casucci, M., Hawkins, R.E., Dotti, G., and Bondanza, A. (2015). Overcoming the toxicity hurdles of genetically targeted T cells. Cancer Immunol. Immunother. *64*, 123–130.
10. Spencer, D.M., Wandless, T.J., Schreiber, S.L., and Crabtree, G.R. (1993). Controlling signal transduction with synthetic ligands. Science *262*, 1019–1024.
11. Straathof, K.C., Pulè, M.A., Yotnda, P., Dotti, G., Vanin, E.F., Brenner, M.K., Heslop, H.E., Spencer, D.M., and Rooney, C.M. (2005). An inducible caspase 9 safety switch for T-cell therapy. Blood *105*, 4247–4254.
12. Di Stasi, A., Tey, S.K., Dotti, G., Fujita, Y., Kennedy-Nasser, A., Martinez, C., Straathof, K., Liu, E., Durett, A.G., Grilley, B., et al. (2011). Inducible apoptosis as a safety switch for adoptive cell therapy. N. Engl. J. Med. *365*, 1673–1683.
13. Zhou, X., Di Stasi, A., Tey, S.K., Krance, R.A., Martinez, C., Leung, K.S., Durett, A.G., Wu, M.F., Liu, H., Leen, A.M., et al. (2014). Long-term outcome after haploidentical stem cell transplant and infusion of T cells expressing the inducible caspase 9 safety transgene. Blood *123*, 3895–3905.
14. Zhou, X., Dotti, G., Krance, R.A., Martinez, C.A., Naik, S., Kamble, R.T., Durett, A.G., Dakhova, O., Savoldo, B., Di Stasi, A., et al. (2015). Inducible caspase-9 suicide gene controls adverse effects from alloreplete T cells after haploidentical stem cell transplantation. Blood *125*, 4103–4113.
15. MacCorkle, R.A., Freeman, K.W., and Spencer, D.M. (1998). Synthetic activation of caspases: Artificial death switches. Proc. Natl. Acad. Sci. USA *95*, 3655–3660.
16. Fan, L., Freeman, K.W., Khan, T., Pham, E., and Spencer, D.M. (1999). Improved artificial death switches based on caspases and FADD. Hum. Gene Ther. *10*, 2273–2285.
17. Tey, S.K., Dotti, G., Rooney, C.M., Heslop, H.E., and Brenner, M.K. (2007). Inducible caspase 9 suicide gene to improve the safety of allodepleted T cells after haploidentical stem cell transplantation. Biol. Blood Marrow Transplant. *13*, 913–924.
18. Bonini, C., Ferrari, G., Verzeletti, S., Servida, P., Zappone, E., Ruggieri, L., Ponzoni, M., Rossini, S., Mavilio, F., Traversari, C., and Bordignon, C. (1997). HSV-TK gene transfer into donor lymphocytes for control of allogeneic graft-versus-leukemia. Science *276*, 1719–1724.
19. Bonini, C., Grez, M., Traversari, C., Ciceri, F., Marktel, S., Ferrari, G., Dinauer, M., Sadat, M., Aiuti, A., Deola, S., et al. (2003). Safety of retroviral gene marking with a truncated NGF receptor. Nat. Med. *9*, 367–369.
20. Maude, S.L., Frey, N., Shaw, P.A., Aplenc, R., Barrett, D.M., Bunin, N.J., Chew, A., Gonzalez, V.E., Zheng, Z., Lacey, S.F., et al. (2014). Chimeric antigen receptor T cells for sustained remissions in leukemia. N. Engl. J. Med. *371*, 1507–1517.
21. Steiner, D., Gelovani, J., Savoldo, B., Robinson, S.N., Decker, W.K., Brouard, N., Najjar, A., Xing, D., Yang, H., Li, S., et al. (2009). Noninvasive bioluminescent imaging demonstrates long-term multilineage engraftment of ex vivo-expanded CD34-selected umbilical cord blood cells. Stem Cells *27*, 1932–1940.
22. Lee, D.W., Gardner, R., Porter, D.L., Louis, C.U., Ahmed, N., Jensen, M., Grupp, S.A., and Mackall, C.L. (2014). Current concepts in the diagnosis and management of cytokine release syndrome. Blood *124*, 188–195.
23. Davila, M.L., Riviere, I., Wang, X., Bartido, S., Park, J., Curran, K., Chung, S.S., Stefanski, J., Borquez-Ojeda, O., Olszewska, M., et al. (2014). Efficacy and toxicity management of 19-28z CAR T cell therapy in B cell acute lymphoblastic leukemia. Sci. Transl. Med. *6*, 224ra25.
24. Jacoby, E., Yang, Y., Qin, H., Chien, C.D., Kochenderfer, J.N., and Fry, T.J. (2016). Murine allogeneic CD19 CAR T cells harbor potent antileukemic activity but have the potential to mediate lethal GVHD. Blood *127*, 1361–1370.
25. Introna, M., Barbui, A.M., Bambacioni, F., Casati, C., Gaipa, G., Borleri, G., Bernasconi, S., Barbui, T., Golay, J., Biondi, A., and Rambaldi, A. (2000). Genetic modification of human T cells with CD20: A strategy to purify and lyse transduced cells with anti-CD20 antibodies. Hum. Gene Ther. *11*, 611–620.
26. Zhao, Y., Wang, Q.J., Yang, S., Kochenderfer, J.N., Zheng, Z., Zhong, X., Sadelain, M., Eshhar, Z., Rosenberg, S.A., and Morgan, R.A. (2009). A herceptin-based chimeric antigen receptor with modified signaling domains leads to enhanced survival of transduced T lymphocytes and antitumor activity. J. Immunol. *183*, 5563–5574.
27. Ciceri, F., Bonini, C., Stanghellini, M.T., Bondanza, A., Traversari, C., Salomoni, M., Turchetto, L., Colombi, S., Bernardi, M., Peccatori, J., et al. (2009). Infusion of suicide-gene-engineered donor lymphocytes after family haploidentical haemopoietic stem-cell transplantation for leukaemia (the TK007 trial): A non-randomised phase I-II study. Lancet Oncol. *10*, 489–500.
28. Ciceri, F., Bonini, C., Marktel, S., Zappone, E., Servida, P., Bernardi, M., Pescarollo, A., Bondanza, A., Peccatori, J., Rossini, S., et al. (2007). Antitumor effects of HSV-TK-engineered donor lymphocytes after allogeneic stem-cell transplantation. Blood *109*, 4698–4707.
29. Arber, C., Abhyankar, H., Heslop, H.E., Brenner, M.K., Liu, H., Dotti, G., and Savoldo, B. (2013). The immunogenicity of virus-derived 2A sequences in immunocompetent individuals. Gene Ther. *20*, 958–962.
30. Kaneko, S., Mastaglio, S., Bondanza, A., Ponzoni, M., Sanvito, F., Aldrighetti, L., Radrizzani, M., La Seta-Catamancio, S., Provasi, E., Mondino, A., et al. (2009). IL-7 and IL-15 allow the generation of suicide gene-modified alloreactive self-renewing central memory human T lymphocytes. Blood *113*, 1006–1015.

31. Kochenderfer, J.N., Dudley, M.E., Carpenter, R.O., Kassim, S.H., Rose, J.J., Telford, W.G., Hakim, F.T., Halverson, D.C., Fowler, D.H., Hardy, N.M., et al. (2013). Donor-derived CD19-targeted T cells cause regression of malignancy persisting after allogeneic hematopoietic stem cell transplantation. Blood *122*, 4129–4139.

32. Wu, C.Y., Roybal, K.T., Puchner, E.M., Onuffer, J., and Lim, W.A. (2015). Remote control of therapeutic T cells through a small molecule-gated chimeric receptor. Science *350*, aab4077.

33. Chang, E.C., Liu, H., West, J.A., Zhou, X., Dakhova, O., Wheeler, D.A., Heslop, H.E., Brenner, M.K., and Dotti, G. (2016). Clonal dynamics in vivo of virus integration sites of t cells expressing a safety switch. Mol. Ther. *24*, 736–745.

34. Vera, J., Savoldo, B., Vigouroux, S., Biagi, E., Pule, M., Rossig, C., Wu, J., Heslop, H.E., Rooney, C.M., Brenner, M.K., et al. (2006). T lymphocytes redirected against the kappa light chain of human immunoglobulin efficiently kill mature B lymphocyte-derived malignant cells. Blood *108*, 3890–3897.

35. Savoldo, B., Ramos, C.A., Liu, E., Mims, M.P., Keating, M.J., Carrum, G., Kamble, R.T., Bollard, C.M., Gee, A.P., Mei, Z., et al. (2011). CD28 costimulation improves expansion and persistence of chimeric antigen receptor-modified T cells in lymphoma patients. J. Clin. Invest. *121*, 1822–1826.

36. Quintarelli, C., Vera, J.F., Savoldo, B., Giordano Attianese, G.M., Pule, M., Foster, A.E., Heslop, H.E., Rooney, C.M., Brenner, M.K., and Dotti, G. (2007). Co-expression of cytokine and suicide genes to enhance the activity and safety of tumor-specific cytotoxic T lymphocytes. Blood *110*, 2793–2802.

37. Imai, C., Mihara, K., Andreansky, M., Nicholson, I.C., Pui, C.H., Geiger, T.L., and Campana, D. (2004). Chimeric receptors with 4-1BB signaling capacity provoke potent cytotoxicity against acute lymphoblastic leukemia. Leukemia *18*, 676–684.

38. Xu, Y., Zhang, M., Ramos, C.A., Durett, A., Liu, E., Dakhova, O., Liu, H., Creighton, C.J., Gee, A.P., Heslop, H.E., et al. (2014). Closely related T-memory stem cells correlate with in vivo expansion of CAR.CD19-T cells and are preserved by IL-7 and IL-15. Blood *123*, 3750–3759.

39. Ramos, C.A., Savoldo, B., Torrano, V., Ballard, B., Zhang, H., Dakhova, O., Liu, E., Carrum, G., Kamble, R.T., Gee, A.P., et al. (2016). Clinical responses with T lymphocytes targeting malignancy-associated κ light chains. J. Clin. Invest. *126*, 2588–2596.

40. Jena, B., Maiti, S., Huls, H., Singh, H., Lee, D.A., Champlin, R.E., and Cooper, L.J. (2013). Chimeric antigen receptor (CAR)-specific monoclonal antibody to detect CD19-specific T cells in clinical trials. PLoS ONE *8*, e57838.

41. Iuliucci, J.D., Oliver, S.D., Morley, S., Ward, C., Ward, J., Dalgarno, D., Clackson, T., and Berger, H.J. (2001). Intravenous safety and pharmacokinetics of a novel dimerizer drug, AP1903, in healthy volunteers. J. Clin. Pharmacol. *41*, 870–879.